2017

3D Bioprinting Human Induced Pluripotent Stem Cell Constructs for In Situ Cell Proliferation and Successive Multilineage Differentiation

Qi Gu
University of Wollongong, Chinese Academy of Sciences, qg863@uowmail.edu.au

Eva Tomaskovic-Crook
University of Wollongong, evatc@uow.edu.au

Gordon G. Wallace
University of Wollongong, gwallace@uow.edu.au

Jeremy Micah Crook
University of Wollongong, jcrook@uow.edu.au

Publication Details

Gu, Q., Tomaskovic-Crook, E., Wallace, G. G. & Crook, J. M. (2017). 3D Bioprinting Human Induced Pluripotent Stem Cell Constructs for In Situ Cell Proliferation and Successive Multilineage Differentiation. Advanced Healthcare Materials, 6 (17), 1700175-1-1700175-11.

3D Bioprinting Human Induced Pluripotent Stem Cell Constructs for In Situ Cell Proliferation and Successive Multilineage Differentiation

Abstract

The ability to create 3D tissues from induced pluripotent stem cells (iPSCs) is poised to revolutionize stem cell research and regenerative medicine, including individualized, patient-specific stem cell-based treatments. There are, however, few examples of tissue engineering using iPSCs. Their culture and differentiation is predominantly planar for monolayer cell support or induction of self-organizing embryoids (EBs) and organoids. Bioprinting iPSCs with advanced biomaterials promises to augment efforts to develop 3D tissues, ideally comprising direct-write printing of cells for encapsulation, proliferation, and differentiation. Here, such a method, employing a clinically amenable polysaccharide-based bioink, is described as the first example of bioprinting human iPSCs for in situ expansion and sequential differentiation. Specifically, There are extrusion printed the bioink including iPSCs, alginate (Al; 5% weight/volume [w/v]), carboxymethyl-chitosan (5% w/v), and agarose (Ag; 1.5% w/v), crosslinked the bioink in calcium chloride for a stable and porous construct, proliferated the iPSCs within the construct and differentiated the same iPSCs into either EBs comprising cells of three germ lineages-endoderm, ectoderm, and mesoderm, or more homogeneous neural tissues containing functional migrating neurons and neuroglia. This defined, scalable, and versatile platform is envisaged being useful in iPSC research and translation for pharmaceuticals development and regenerative medicine.

Disciplines

Engineering | Physical Sciences and Mathematics

Publication Details

Gu, Q., Tomaskovic-Crook, E., Wallace, G. G. & Crook, J. M. (2017). 3D Bioprinting Human Induced Pluripotent Stem Cell Constructs for In Situ Cell Proliferation and Successive Multilineage Differentiation. Advanced Healthcare Materials, 6 (17), 1700175-1-1700175-11.

DOI: 10.1002/adhm.201700175
Article type: Full Paper

Title 3D bioprinting human induced pluripotent stem cell constructs for *in situ* cell proliferation and successive multi-lineage differentiation

*Author(s), and Corresponding Author(s)** Qi Gu, Eva Tomaskovic-Crook, Gordon G. Wallace*, and Jeremy M. Crook*

Dr. Q. Gu, Dr. E. Tomaskovic-Crook, Prof. G. G. Wallace, Assoc. Prof. J. M. Crook
ARC Centre of Excellence for Electromaterials Science, Intelligent Polymer Research Institute, AIIM Facility, Innovation Campus, University of Wollongong, Squires Way, Fairy Meadow, New South Wales 2519, Australia
E-mail: jcrook@uow.edu.au; gwallace@uow.edu.au
Dr. E. Tomaskovic-Crook, Assoc. Prof. J. M. Crook
Illawarra Health and Medical Research Institute, University of Wollongong, Wollongong, New South Wales 2522, Australia
Dr. Q. Gu
State Key Laboratory of Stem Cell and Reproductive Biology, Institute of Zoology, Chinese Academy of Sciences, Beijing, 100101, P.R. China
Assoc. Prof. J. M. Crook
Department of Surgery, St Vincent's Hospital, The University of Melbourne, Fitzroy, Victoria 3065, Australia

Keywords: 3D bioprinting, induced pluripotent stem cells, endoderm, ectoderm, mesoderm, neural tissue

The ability to create three-dimensional (3D) tissues from induced pluripotent stem cells (iPSCs) is poised to revolutionize stem cell research and regenerative medicine, including individualized, patient-specific stem cell-based treatments. There are, however, few examples of tissue engineering using iPSCs. Their culture and differentiation is predominantly planar for monolayer cell support or induction of self-organizing embryoids (EBs) and organoids. Bioprinting iPSCs with advanced biomaterials promises to augment efforts to develop 3D tissues, ideally comprising direct-write printing of cells for encapsulation, proliferation, and differentiation. Here such a method, employing a clinically-amenable polysaccharide-based bioink, is described as the first example of bioprinting human iPSCs for *in situ* expansion and sequential differentiation. Specifically, we have extrusion printed the bioink including iPSCs, alginate (Al; 5% weight/volume [w/v]), carboxymethyl-chitosan (CMC; 5% w/v) and agarose

(Ag; 1.5% w/v), crosslinked the bioink in calcium chloride for a stable and porous construct, proliferated the iPSCs within the construct and differentiated the same iPSCs into either EBs comprising cells of three germ lineages – endoderm, ectoderm, and mesoderm, or more homogeneous neural tissues containing functional migrating neurons and neuroglia. This defined, scalable and versatile platform is envisaged being useful in iPSC research and translation for pharmaceuticals development and regenerative medicine.

1. Introduction

Human iPSCs, like embryonic stem cells, have the ability to self-renew for large-scale expansion whilst maintaining the capacity to differentiate to all cell types (~200) of the human body.[1-3] These qualities, together with the potential for autologous application, make iPSCs compelling candidates for cell replacement therapies, tissue and organ engineering, and pharmacology and toxicology screening.

Since their discovery a decade ago, the development of culture protocols for human iPSCs has primarily focused on clinical-compliance,[4] cell line stability,[5] and efficiency of differentiation to desired cell lineages,[6] all the while retaining conventional monolayer (2D) culture. Recent interest in recapitulating the 3D cytoarchitecture of native tissues *in vitro* to better simulate cell behavior *in vivo*, together with advances in fabricating bioactive, mechanically tunable and biocompatible materials are driving the application of 3D configured biomaterials for stem cell research and therapy.[7, 8] For example, by mimicking important features of a target tissue including the extracellular microenvironment, 3D-biomaterials have the potential to instruct cell fate and function in ways not previously attainable.[9] Therefore, although still exploratory, we envisage the synergism of stem-cell biology and 3D-biomaterial technology being influential in iPSC-based research and translation.

The small numbers of 3D systems for iPSC culture reported to date rely on the ability of iPSCs to self-organise when seeded onto or cast within supporting material such as conventional tumor-derived Matrigel® basement membrane or more defined polymeric scaffolds.[10-13] An alternative although previously untested approach to bioengineering 3D iPSC constructs is to apply advanced 3D bioprinting for direct-write (or co-) printing of stem cells together with biomaterial to reproducibly generate tissue of a desired architecture. Co-printing represents a single-step approach to rapidly fabricate a 3D cellularized construct whereby iPSCs are immediately integrated with biomaterials by encapsulation for direct and complete contact with extracellular elements that more closely mimic the native cell microenvironment.

Here we describe a body of work related to iPSC printing following on from our previously published report of human neural stem cell (NSC) printing.[14] By utilizing the defined clinically-amenable polysaccharide-based bioink containing Al, CMC and Ag, we have optimized extrusion printing of iPSCs (**Figure 1**A), enabling for the first time their maintenance as self-renewing stem cells within the printed construct after gelation. Cell proliferation endures for at least 9 days post-printing (Figure 1B) and stem cells can be uniquely differentiated *in situ* to self-assembling 3D cell aggregates called embryoid bodies with cells constituting all three primitive germ layers – mesoderm, ectoderm and endoderm (Figure 1C). Following transition of the printed iPSC constructs to neural induction/differentiation media, more homogeneous neural tissues can be generated with neurons and supporting neuroglia (Figure 1D). Neurons are active, form synapses, participate in network activity and show migratory behavior within a construct.

Our findings affirm the efficacy of our previously described bioprinting platform for generating 3D tissues from human stem cells. Consistent with the biomaterials used providing a uniform bioink consistency and suitable viscosity (requiring an extrusion force of around 8.5 N)[14], cells can be printed for homogenous distribution and high viability, with support

sustained after ionic-crosslinking due to previously demonstrated mechanical properties including high gel porosity for permeability to bioactive factors, and stiffness (indentation modulus < 5 kPa)[14] for enduring biocompatibility. Having now adapted the platform for human iPSC printing and differentiation, we have verified its versatility for generating both neural and non-neural tissues including amenability to "notoriously difficult to culture" cell types such as human iPSCs.[15, 16]

2. Results and Discussion

2.1 iPSC bioprinting, survival and *in situ* proliferation

Extrusion printing of optimal iPSC-laden bioink resulted in the generation of scaffolds containing uniformly distributed stem cells throughout (**Figure 2**A, B and C). Encapsulated cells were viable with negligible cell death apparent immediately after ink gelation by ionic-crosslinking, persisting through extended culture in excess of 7 days (Figure 2A). iPSCs showed characteristic pluripotent cell morphology, similar to embryonic stem cells (ESCs), being round in shape with large nuclei and sparse cytoplasm. During the course of maintaining constructs for stem cell expansion, iPSCs proliferated to form aggregates of cells culminating in large spheroids by day 7. Spheroids could be clearly seen abutting the lumen of scaffolds and dispersed throughout the gel. The phenomenon of spheroid formation is consistent with colony formation during conventional 2D culture, but with spheroids reflecting well-defined clusters of tightly packed cells within a 3D system as compared to classical (2D) sharp-edged, flat, tightly packed colonies.[16]

iPSC growth profiling showed cell proliferation increased from the time of printing and peaked at day 9 (Figure 2D). The observed peak and subsequent decrease is consistent with contact inhibition as cell cultures reach confluency within the constructs. Inhibition of cellular growth, division and motility is characteristic of mammalian cells when in close

contact with each other. Therefore, as iPSCs reached a high density by proliferating after printing, cessation of cell growth would reasonably be expected.

Flow cytometry of iPSCs extracted from printed constructs after 10 days culture revealed ubiquitous expression of pluripotency cell markers OCT4, SOX2, TRA-1-60 and SSEA4, consistent with a persistent pluripotent stem cell state (Figure 2E; Figure S1, Supporting Information). Cell pluripotency was also confirmed by formation of prototypical iPSC-colonies from similarly extracted spheroids that were sub-cultured by conventional 2D-planar method (Figure 2F). Moreover, immunophenotyping with confocal microscopy demonstrated iPSC-spheroids within constructs expressed OCT4, SOX2, SSEA4, and TRA-1-60 (**Figure 3**).

2.2 *In situ* differentiation of iPSCs to EBs comprising cells of three germ lineages – endoderm, ectoderm, and mesoderm

The differentiation potential of printed constructs was initially investigated by directing 3D bioprinted iPSCs to form EBs within constructs. EBs are 3D cell aggregates, which mimic many of the hallmarks of embryonic development. As EBs develop, differentiated cell phenotypes of all three germ lineages arise.[17] Therefore, in addition to demonstrating multi-lineage cell and tissue formation, the induction of EBs represents another test of pluripotency.

EBs formed within 3D constructs following modification of the iPSC culture media to basic fibroblast growth factor (bFGF)-free medium 5 days post-printing. They displayed archetypal morphology, with radiating and retracting projections (**Figure 4**A; Video S1, Supporting Information). The observed projections are consistent with EBs often exhibiting tissue-like structures, such as the patterning of neurite extensions indicative of neuron organization.[18] Notwithstanding the evidence for neural cell lineage, assessment of gene expression of extracted EBs by reverse-transcription quantitative PCR (RT-qPCR) confirmed downregulation of pluripotency markers *OCT4, NANOG, TDGF1, and UTF1* compared to

undifferentiated EB-controls, with increased expression of endodermal (*H19* and *PDX1*), mesodermal (*HAND1* and *IGF2*) and ectodermal (*NES* and *TUBB-3*) markers confirming iPSC differentiation to all germ lineages (Figure 4B and C). Taken together, these data substantiate the potential to form multiple cell and tissue types within and from the bioprinted constructs. Secondarily, the results are consistent with having maintained iPSC status for the period of preserving constructs in culture after printing, prior to differentiation.

Interestingly, despite affirming pluripotency of undifferentiated iPSCs, and loss of pluripotency and multi-lineage cell induction with differentiation, it is notable that gene expression was not enhanced for every marker of differentiation in 3D bioprinted constructs compared to conventional 2D differentiation. Specifically, H19, Hand-1, NES and TUBB3 were higher for printed constructs, but PDX1 and IGF2 were not. Modifying the properties of the bioink and parameters of printing and gelation could enable fine-tuning of a cohort of markers associated with a particular tissue lineage. However, the specific adjustments to method will depend on the cell types required, with desired (and potentially undesired) contemporaneous effects on initial stem cell support also needing to be considered. Accordingly, there may be a trade-off between iPSC support and differentiated cell and tissue support. Notwithstanding, and importantly, our current described protocol enables apposite stem cell support, measurable endodermal, ectodermal and mesodermal cell induction and support, while concomitantly affording robust neural cell and tissue induction and maintenance further described below.

2.3 Directed differentiation of 3D bioprinted iPSC constructs to neural tissues

While without specific medium supplements pluripotent stem cells have a tendency to differentiate to derivatives of the three germ lineages, alternative media compositions (including the use of defined growth factor additives) can promote differentiation toward one or another lineage.[6] Given our earlier work on generating neural tissues using bioprinted NSCs, we sought to similarly generate neural tissue from the 3D bioprinted iPSCs.

Differentiation involved an intermediate progenitor phase by culturing constructs in neural induction medium for 2-3 weeks from the third day after printing, followed by differentiation (using further modified medium including brain-derived neurotrophic factor; BDNF) into mature cells with phenotypes representative of different neuronal subtypes and supporting neuroglia. Consistent with forming iPSC-derived neural progenitors, immunophenotyping of constructs following 17 days of neural induction (20 days post-printing) revealed cells expressing neural progenitor markers PAX6 and NESTIN (**Figure 5**). Subsequent analysis of further differentiated (> 30 days) constructs confirmed maturation to tissues comprising cells expressing pan-neuronal markers microtubule-associated protein 2 (MAP2; **Figure 6**A and D) and class III beta-tubulin protein (TUBB3; Figure 6C), as well as radial glial and astrocyte marker glial fibrillary acid protein (GFAP; Figure 6B and D) and presynaptic vesicle glycoprotein synaptophysin (Figure 6C). MAP2-expressing neurons often abutted the neuroglia (Figure 6D) and synaptophysin colocalized to neurites and neuronal cell soma, including longer neurite projections between neuronal cell clusters (Figure 6C).

Further immunocytochemistry together with RT-qPCR substantiated discrete neural cell subtypes including gamma-aminobutyric acid (GABA) expressing neurons (Figure 6E), corroborated by transcript for *NKX2-1*, as well as serotonergic marker *PET1* and oligodendrocyte lineage transcription factor 2 (*OLIG2*) (**Figure 7**). RT-qPCR also confirmed increased transcript for *NES*, *TUBB3* and *GFAP*, with highest levels of expression for 3D differentiated iPSCs compared to undifferentiated controls and 2D differentiated iPSCs, as well as concomitant downregulation of pluripotency markers *OCT4*, *NANOG*, and *SOX2* (Figure 7). Finally, consistent with the presence of GABAergic neurons, neurons displayed recurrent increases in extracellular calcium concentration in response to GABA receptor-A antagonist bicuculline (**Figure 8A**; Video S2, Supporting Information). Functionality was also supported by neuronal cell migration within constructs, including characteristic long and dynamic leading processes (Figure 8B; Video S3, Supporting Information). Migrating

neurons generally exhibit a leading process, with some being branched and others single.[19] The example presently shown is a neuron with a "relatively unbranched process" that appears to retract and extend and a tip that clearly moves forward as the cell traverses the construct (Video S3, Supporting Information).

Taken together, the above findings verify the ability to differentiate iPSCs within the bioprinted constructs and in particular their conversion to functional neural cells for 3D neural tissue formation.

3. Conclusion

There are a number of different yet-to-be-tested bioprinting platforms that may be suitable for 3D iPSC deposition including inkjet-based[20], laser-assisted[21] and electrospray[22, 23] bioprinting. While it will be important to determine the utility of these platforms, our work represents the first example of bioprinting iPSCs for ensuing culture and expansion within a 3D construct. In addition, we were able to sequentially differentiate printed iPSCs *in situ* to multiple lineages representative of all three germ layers – mesoderm, ectoderm and endoderm, as well as form more homogeneous neural tissues. To the best of our knowledge, the only other example of bioprinting pluripotent stem cells and more specifically iPSCs involved printing with cell culture media for subsequent immediate testing of post-printing cell viability and pluripotency.[24] The iPSCs were neither 3D-printed with supporting biomaterial, nor 3D-cultured or -differentiated following printing.

We have overcome reputed difficulties with maintaining and differentiating iPSCs, in spite of printing, by using a bioink with well-characterised and inexpensive components, having optimal viscosity for initial cell support during printing, and continuing support after printing and gelation. Al, CMC and Ag are widely available and used for clinical purposes, each having inherent qualities beneficial to the bioprinting process and/or cell survival.[14, 25, 26] While we have previously detailed their individual and combined properties, briefly, Al

enabled cyotcompatible gelation using calcium chloride, CMC afforded favorable porosity and related permeability, and Ag provided the rheological properties required for printing.[14] Moreover, CMC has other known beneficial properties such as high moisture retention, low inflammatory, toxicity and antimicrobial responses, and promotion of cell adhesion, migration and proliferation.[27, 28]

In summary, the ability to 3D print human iPSCs to then expand and generate cells of different lineages provides an unprecedented opportunity to form different, authentic and renewable body tissues. To this end, the present body of work represents a first important step, with further refinement of method expected to enhance tissue identity, architecture and function to better model development and diseases, for pharmaceuticals screening and assessing *in vivo* function and safety in animal models towards transplantation therapies.

4. Experimental Section

iPSC culture and differentiation: Working stocks of human iPSCs were maintained as 2D cultures in 5% CO_2 at 37°C, mTeSR™1 (STEMCELL Technologies) on Matrigel® basement membrane matrix (Corning) in 6-well plates (Greiner Bio-One). Cells were passaged when colony centres became dense by incubation with 0.02% disodium ethylenediamine tetraacetate (EDTA; Sigma-Aldrich) for 3 min and fluxing with a pipette, followed by a 1:4-1:6 split. To form EBs, iPSC colonies were extracted non-enzymatically and transferred to fresh culture plates for non-adherent suspension culture in the medium without bFGF (Peprotech).

For 3D printed hiPSC culture and differentiation, mTESR™1 was again used for hiPSC expansion, and medium (DMEM/F12, Life Technologies) supplemented with 20% KnockOut™ Serum Replacement (Life Technologies), 1×MEM non-essential amino acids solution (NEAA; 100x stock, Gibco) and 55 μM β-mercaptoethanol (Gibco) without bFGF was used for induction of EBs. For the former culture medium was supplemented with 5 μM

rock inhibitor Y-27632 (STEMCELL Technologies) for the first 3 days of culture, while for EB formation, medium was changed to bFGF-free medium on the fifth day post-printing.

For 3D iPSC differentiation to neural lineage, neural induction medium (comprising DMEM/F12 (1:1; Gibco) supplemented with 1% N-2 supplement (Gibco), 2 µg/ml heparin (Sigma-Aldrich) and MEM NEAA was applied every 2 – 3 days from the third day after printing, and then 2-3 weeks later, the medium was changed to neuronal differentiation medium containing 2 parts DMEM F-12 : 1 part Neurobasal medium (Gibco) supplemented with 2% StemPro Neural Supplement (Gibco), 0.5 % N-2 Supplement and 50 ng/ml brain-derived neurotrophic factor (BDNF; Peprotech) for 3 weeks culture.

Bioink preparation and bioprinting: The bioink was prepared as previously described.[14] Briefly, agarose (Ag; Astral Scientific Pty Ltd) was dissolved in phosphate-buffered saline (PBS; pH7.4; Sigma-Aldrich) by heating in a microwave oven to give 1.5% (w/v), followed by addition of alginate (Al; MW ~50,000 Da, M/G ratio of 1.67, viscosity of 100–300 cP for 2 w/w solution, 25°C; Sigma-Aldrich) and carboxymethyl-chitosan (CMC; Shanghai DiBai Chemicals) to give 5% (w/v). After 1 hr stirring at 60 °C, the final solution was cooled to room temperature (RT) and $4x10^7$ iPSCs were added per 0.5 ml bioink.

Bioprinting was performed with a 3D-Bioplotter® System (EnvisionTEC) fitted with a 55CC barrel (Nordson Australia) and 200 µm printing nozzle (Nordson Australia). Bioink samples were loaded into the barrel and centrifuged at 300 g at 15 ^{o}C for 1 min to remove air bubbles, followed by printing onto autoclaved glass slides. After printing, scaffolds were immersed in 2% (w/v) calcium chloride for 10 min to crosslink. After gelation, the constructs were rinsed 3 times in culture medium followed by 2 x 10 min washes and incubation in fresh culture medium for 1 h to remove excess calcium ions.

Scanning Electron Microscopy (SEM): For SEM of printed constructs, samples were submersed in hiPSC culture media for 24 hr, freeze dried overnight using a Alpha 2-4 LD freeze dryer (Christ), then coated with 20 nm gold using a sputter coater (Edwards), and kept

desiccated until analysed. SEM was performed using a JSM-7500FA LV Scanning Electron Microscope. For studies of internal structure, samples were fixed with 3.7% paraformaldehyde (PFA, Fluka) for 30 min, immersed in liquid nitrogen for 60 seconds, and then freeze-fractured using a cold razor blade. The fractured samples were immediately observed on the JSM-6490 LV Scanning Electron Microscope (Jeol).

Live/dead iPSC analysis: Calcein AM (5 μg/ml, Life technologies) and propidium iodide (PI, 5 μg/ml, Life technologies) were used to detect live and dead cells respectively. Briefly, constructs were incubated at 37 ºC with Calcein AM for 10 min, followed by PI for 1 min. A Leica TSC SP5 II confocal microscope was used for image acquisition, with images from a minimum of five optical planes per construct merged (to capture the maximal projection of whole cell aggregates) for analysis using Fiji (Image J) software.[29] Three independent samples were evaluated for each gel composition. Depth coding of constructs was performed using the 3D Projection Tool in Leica Application Suite (LAS AF) software (Leica).

Immunocytochemistry: Samples were fixed with 3.7 % paraformaldehyde (PFA) in PBS for 30 min at RT. Samples were then blocked and permeabilized overnight with 5% (v/v) donkey serum (Merck Millipore) in PBS containing 0.3% (v/v) Triton X-100 (Sigma-Aldrich) at 4 °C. Samples were subsequently incubated with primary antibodies against OCT4 (mouse, 1:200, STEMCELL Technologies), SSEA4 (mouse, 1:200, STEMCELL Technologies), TRA-1-60 (mouse, 1:200, STEMCELL Technologies), PAX6 (rabbit, 1:100, Sigma-Aldrich), nestin (mouse, 1:100; Invitrogen), synaptophysin (rabbit, 1:200; Merck Millipore), TUBB3 as recognised by the TuJ1 antibody (Chicken, 1:200, Merck Millipore) and GABA (rabbit, 1:200; Sigma-Aldrich) or fluorescence conjugated antibodies GFAP (mouse, 1:100; Cell Signalling), MAP2 (mouse, 1:100, Merck Millipore), SOX2 (rabbit, 1:100; Cell Signalling) at 4 °C overnight. On the second day, samples were rinsed with 0.1% Triton X-100 in PBS three times and samples with unconjugated primary antibody were incubated with species-specific Alexa Fluor tagged secondary antibody (1:1000; Invitrogen) for 1 hr at 37 °C. Nuclei were

labelled with 4',6-diamidino-2-phenylindole (DAPI, 10 μg/ml; Invitrogen) at RT for 10 min and Prolong Gold antifade reagent (Invitrogen) was employed to preserve fluorescence signal. Samples were mounted onto glass coverslips using Aquamount (ThermoScientific) and imaged with a Leica TSC SP5 II confocal microscope. Images were collected and analysed using Leica Application Suite AF (LAS AF) software (Leica).

iPSC Proliferation Analysis: PrestoBlue™ (Invitrogen) cell viability reagent was used for iPSC proliferation studies, according to the manufacturer's instructions. Briefly, at each time point measured, three cell-laden constructs were incubated with the reagent in culture medium for 1 hr at 37 ^{o}C. For each construct, 100 μl supernatant was transferred to a well of a 96-well plate and screened by a microplate reader (POLARstar Omega) to read fluorescence intensity. Constructs were subsequently rinsed in culture medium and returned to culture, with the process repeated for each time point until the study was completed.

Real-time quantitative PCR (RT-qPCR): For RNA isolation, conventional 2D cultured iPSCs, EBs and neural cells were treated with TRIzol™ Reagent (Invitrogen). 3D gel-encapsulated cells were first treated with 0.05 M EDTA for 10 min, fluxed with a pipette, followed by centrifugation at 600 g for 5 min. TRIzol™ Reagent was then used to isolate total RNA and isopropanol (Chem-Supply) was used to precipitate RNA. The purity and quantity of the RNA was assessed using a NanoDrop™ 2000c Spectrophotometer (Thermo Scientific). cDNA was synthesized from the RNA using random primers. A Gotaq 2-step RT-qPCR Kit (Promega) and Bio-Rad CFX Real Time PCR instrument were used to perform RT-qPCR. CFX software was used to analyse data according to delta-delta Ct method.[30] Primer sequence information is provided in **Table S1** (Supporting Information).

Flow cytometry: 3D gel-encapsulated iPSC-spheroids were extracted from the 3D structures as described above for RT-qPCR. For both extracted spheroids and 2D cultured iPSCs, cells were digested in 0.02% EDTA for 5 min and 10 min respectively, triturated, and passed through a 40 μm sieve to generate single cell preparations. After trituration, single cells were

pelleted followed by centrifugation at 300 g for 5 min and fixed with 3.7% paraformaldehyde solution in PBS on ice for 10 min. After 2 washes in 0.1% (v/v) Triton X-100 in PBS, cells were resuspended in blocking buffer (5% Goat Serum plus 0.3% Triton-x-100 in PBS) and placed on ice for 30 min. Cells were then incubated with primary antibodies for OCT4, SSEA4 and TRA-1-60 described above and SOX2 (rabbit, 1:200; STEMCELL Technologies), and diluted in wash buffer on ice for 30 min. Following a further 2-3 washes, species-specific secondary antibodies conjugated with Alexa Fluor (1:1000; Invitrogen) and diluted in blocking buffer were applied for 30 min on ice in the dark. Cells were then washed again before being resuspended in 2% FBS/PBS and analysed by a Accuri C6 flow cytometer (BD Biosciences).

Calcium imaging: Calcium imaging was performed by incubating samples with 2 µM Fluo-4 (Life Technologies) in fresh culture medium for 30 min at 37ºC, followed by washing in Tyrode's solution (5 mM KCl, 129mM NaCl, 2mM CaCl2, 1mM MgCl2, 30mM D-Glucose and 25 mM HEPES, pH 7.4).[31] The samples were mounted onto coverslips and observed on a Leica TSC SP5 II confocal microscope. The data were collected and quantified using LAS AF software (Leica). To induce intracellular calcium, GABA(A) receptor antagonist Bicuculline (50 µM; Sigma-Aldrich) was added with Tyrode's solution for 3 min followed by further imaging.

Supporting Information

Supporting Information is available from the Wiley Online Library or from the author.

Acknowledgements

JMC, GGW and QZ conceived the study. JMC, QG and ETC planned and/or executed experiments. JMC wrote the manuscript with contributions from all authors. The authors wish to acknowledge funding from the Australian Research Council (ARC) Centre of Excellence Scheme (CE140100012), the use of facilities at the University of Wollongong Electron

Microscopy Centre, support of the Australian National Fabrication Facility (ANFF) – Materials Node, and assistance provided by Ms. Situ Abdul Rahim with Flow Cytometry. Professor Gordon Wallace acknowledges the support of the ARC through an ARC Laureate Fellowship (FL110100196).

Received: ((will be filled in by the editorial staff))
Revised: ((will be filled in by the editorial staff))
Published online: ((will be filled in by the editorial staff))

[1] J. Yu, M. A. Vodyanik, K. Smuga-Otto, J. Antosiewicz-Bourget, J. L. Frane, S. Tian, J. Nie, G. A. Jonsdottir, V. Ruotti, R. Stewart, Slukvin, II, J. A. Thomson, *Science* **2007**, *318*, 1917.

[2] J. A. Thomson, J. Itskovitz-Eldor, S. S. Shapiro, M. A. Waknitz, J. J. Swiergiel, V. S. Marshall, J. M. Jones, *Science* **1998**, *282*, 1145.

[3] K. Takahashi, K. Tanabe, M. Ohnuki, M. Narita, T. Ichisaka, K. Tomoda, S. Yamanaka, *Cell* **2007**, *131*, 861.

[4] J. M. Crook, T. T. Peura, L. Kravets, A. G. Bosman, J. J. Buzzard, R. Horne, H. Hentze, N. R. Dunn, R. Zweigerdt, F. Chua, A. Upshall, A. Colman, *Cell Stem Cell* **2007**, *1*, 490.

[5] J. J. Buzzard, N. M. Gough, J. M. Crook, A. Colman, *Nature Biotechnology* **2004**, *22*, 381.

[6] J. M. Crook, in Human Stem Cell Technology and Biology: A Research Guide and Laboratory Manual., (Eds: M. B. G.S. Stein, M.X. Luong, M.J. Shi, K.P. Smith, P. Vasquez), Wiley Blackwell, **2011**, 289.

[7] T. P. Kraehenbuehl, R. Langer, L. S. Ferreira, *Nature Methods* **2011**, *8*, 731.

[8] X. Wu, S. Mahalingam, S.K. VanOosten, C. Widom, C. Tamerler, M. Edirisinghe. *Macromolecular Bioscience* **2017,** *17*, 1600270.

[9] W. L. Murphy, T. C. McDevitt, A. J. Engler, *Nature Materials* **2014**, *13(6)*, 547.

[10] M. A. Lancaster, M. Renner, C. A. Martin, D. Wenzel, L. S. Bicknell, M. E. Hurles, T. Homfray, J. M. Penninger, A. P. Jackson, J. A. Knoblich, *Nature* **2013**, *501*, 373.

[11] J. Jo, Y. Xiao, A. X. Sun, E. Cukuroglu, H. D. Tran, J. Goke, Z. Y. Tan, T. Y. Saw, C. P. Tan, H. Lokman, Y. Lee, D. Kim, H. S. Ko, S. O. Kim, J. H. Park, N. J. Cho, T. M. Hyde, J. E. Kleinman, J. H. Shin, D. R. Weinberger, E. K. Tan, H. S. Je, H. H. Ng, *Cell Stem Cell* **2016**, *19*, 248.

[12] B. A. Lindborg, J. H. Brekke, A. L. Vegoe, C. B. Ulrich, K. T. Haider, S. Subramaniam, S. L. Venhuizen, C. R. Eide, P. J. Orchard, W. Chen, Q. Wang, F. Pelaez, C. M. Scott, E. Kokkoli, S. A. Keirstead, J. R. Dutton, J. Tolar, T. D. O'Brien, *Stem Cells Translational Medicine* **2016**, *5*, 970.

[13] Y. Lei, D. V. Schaffer, *Proceedings of the National Academy of Sciences of the United States of America* **2013**, *110*, E5039.

[14] Q. Gu, E. Tomaskovic-Crook, R. Lozano, Y. Chen, R. M. Kapsa, Q. Zhou, G. G. Wallace, J. M. Crook, *Advanced Healthcare Materials* **2016**, *5*, 1429.

[15] S. Konagaya, T. Ando, T. Yamauchi, H. Suemori, H. Iwata, *Scientific Reports* **2015**, *5*, 16647.

[16] R. Kato, M. Matsumoto, H. Sasaki, R. Joto, M. Okada, Y. Ikeda, K. Kanie, M. Suga, M. Kinehara, K. Yanagihara, Y. Liu, K. Uchio-Yamada, T. Fukuda, H. Kii, T. Uozumi, H. Honda, Y. Kiyota, M. K. Furue, *Scientific Reports* **2016**, *6*, 34009.

[17] G. M. Keller, *Current Opinion in Cell Biology* **1995**, *7*, 862.

[18] A. M. Bratt-Leal, R. L. Carpenedo, T. C. McDevitt, *Biotechnology Progress* **2009**, *25*, 43.

[19] J. A. Cooper, T*he Journal of Cell Biology* **2013**, *202*, 725.

[20] D.F.E. Ker, B. Chu, J.A. Phillippi, B. Gharaibeh, J. Huard, L.E. Weiss, P.G. Campbell. *Biomaterials* **2011**, *32*, 3413.

[21] W. Wang, G. Li, Y. Huang. *Journal of Manufacturing Science and Engineering* **2009**, *131*, 051013.

[22] S.N. Jayasinghe, P.A. Eagles, A.N. Qureshi. Biotechnology Journal **2006**, *1(1)*, 86.

[23] Y. Xin, G. Chai, T. Zhang, X. Wang, M. Qu, A. Tan, M. Bogari, M. Zhu, L. Lin, Q. Hu, Y. Liu, Y. Zhang. *Biomedical Reports* **2016**, *5(6)*, 723.

[24] A. Faulkner-Jones, C. Fyfe, D. J. Cornelissen, J. Gardner, J. King, A. Courtney, W. Shu, *Biofabrication* **2015**, *7*, 044102.

[25] K. Y. Lee, D. J. Mooney, *Progress in Polymer Science* **2012**, *37*, 106.

[26] L. Upadhyaya, J. Singh, V. Agarwal, R. P. Tewari, *Carbohydrate Polymers* **2013**, *91*, 452.

[27] P. R. Sivashankari, M. Prabaharan, *International Journal of Biological Macromolecules* **2016**, *93*, 1382.

[28] V. Patrulea, L. A. Applegate, V. Ostafe, O. Jordan, G. Borchard, *Carbohydrate Polymers* **2015**, *122*, 46.

[29] J. Schindelin, I. Arganda-Carreras, E. Frise, V. Kaynig, M. Longair, T. Pietzsch, S. Preibisch, C. Rueden, S. Saalfeld, B. Schmid, J. Y. Tinevez, D. J. White, V. Hartenstein, K. Eliceiri, P. Tomancak, A. Cardona, *Nature Methods* **2012**, *9*, 676.

[30] K. J. Livak, T. D. Schmittgen, *Methods* **2001**, *25*, 402.

[31] M. W. Radomski, R. M. Palmer, S. Moncada, *Proceedings of the National Academy of Sciences of the United States of America* **1990**, *87*, 10043.

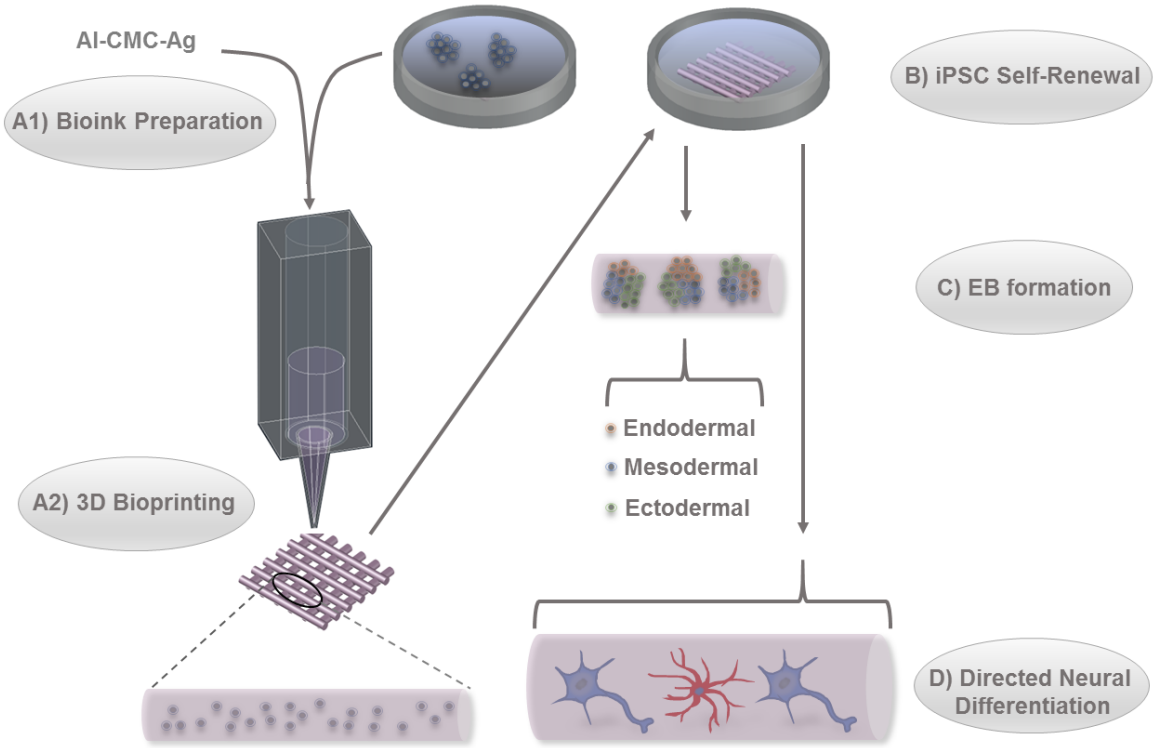

Figure 1. Schematic of the method for extrusion printing of iPSCs for 3D culture and differentiation. A) Bioink is prepared by suspending iPSCs with clinically-amenable polysaccharides Al (5% w/v), CMC (5% w/v) and Ag (1.5% w/v), followed by bioprinting and ionic-crosslinking for gelation. B) 3D iPSC-laden scaffolds are maintained in iPSC-culture medium for stem cell proliferation/self-renewal within the printed construct. C) iPSCs can be differentiated *in situ* to self-assembling 3D EBs comprising cells of all three primitive germ layers – mesoderm, ectoderm and endoderm, or D) more homogeneous neural tissues using neural induction and differentiation media. Neural constructs incorporate functional (including migrating) neurons and supporting neuroglia.

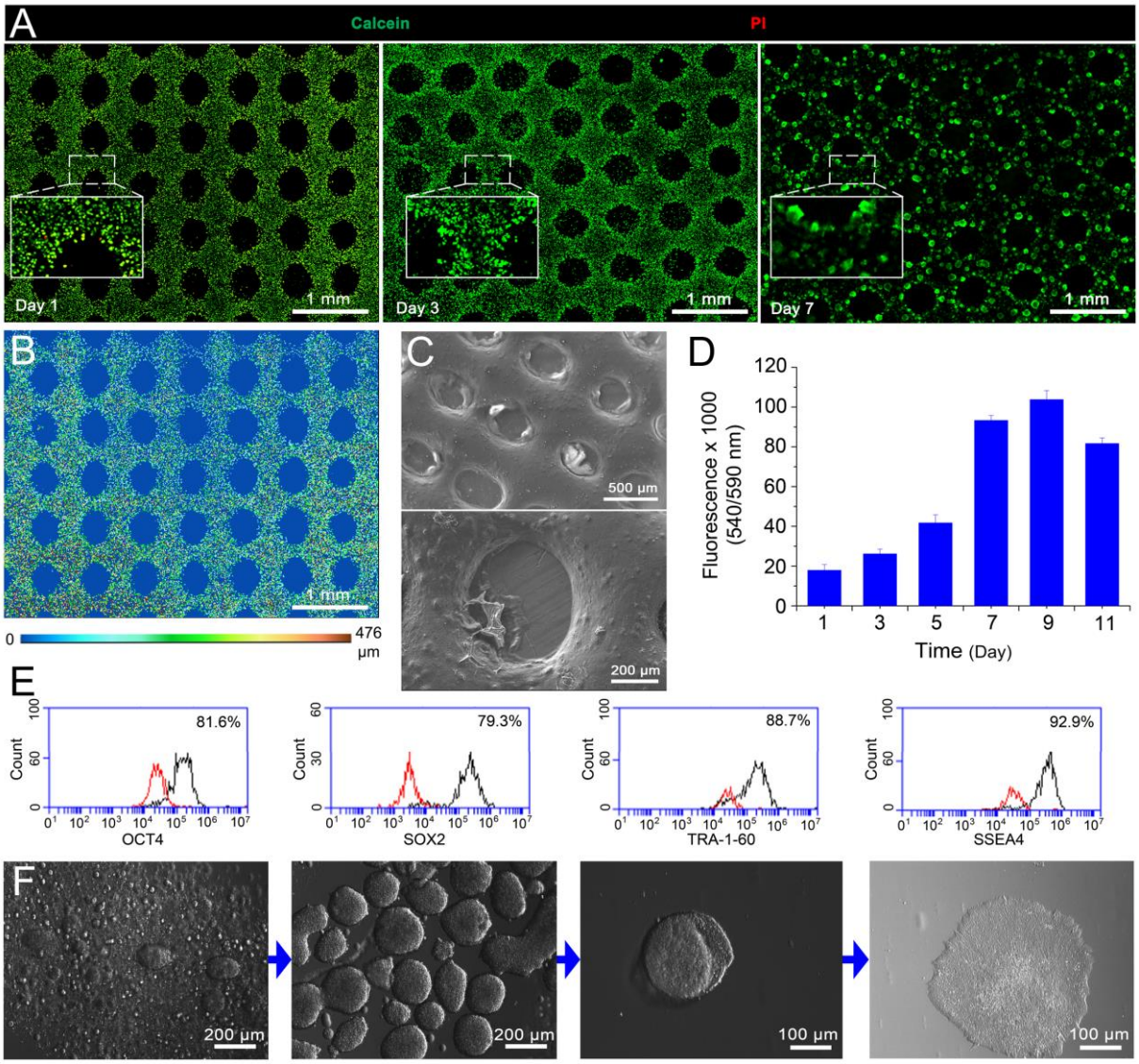

Figure 2. Survival and proliferation of 3D bioprinted iPSCs, and cell sub-culture following extraction post-printing. A) Live (Calcein AM) and dead (Propidium iodide; PI) iPSC staining within a printed construct at days 1, 3 and 7 post-printing. Initially encapsulated iPSCs are visible as evenly distributed single cells, with aggregates of cells increasingly apparent over time. By day 7 cell aggregates appear as large spheroids, abutting the lumen of scaffolds, though dispersed throughout the gel. B) Depth coding of iPSCs along the Z-axis of a 3D printed construct (0 – 476 µm). C) SEM images of as-printed scaffold, inclusive of iPSCs. D) Time course of live (PrestoBlue cell viability indicator) iPSC content of gel constructs up to day 11 after printing (mean ± S.D.; *n* = 3). One-way ANOVA with Bonferroni post hoc test. *P < 0.0001 (day 7 vs day 1). E) Flow cytometry of iPSCs extracted from 3D constructs 10 days post-printing and expressing Oct4, SOX2, TRA-1-60 and SSEA4 (black histograms). Red histograms indicate the isotype controls. (See also Figure S1, Supporting Information). F) Following extraction of iPSC-spheroids from 3D printed constructs (ie. 11 days post-printing) they could be recovered for conventional planar sub-culture forming classical iPSC-colonies on Matrigel® basement membrane matrix. Scale bars as indicated.

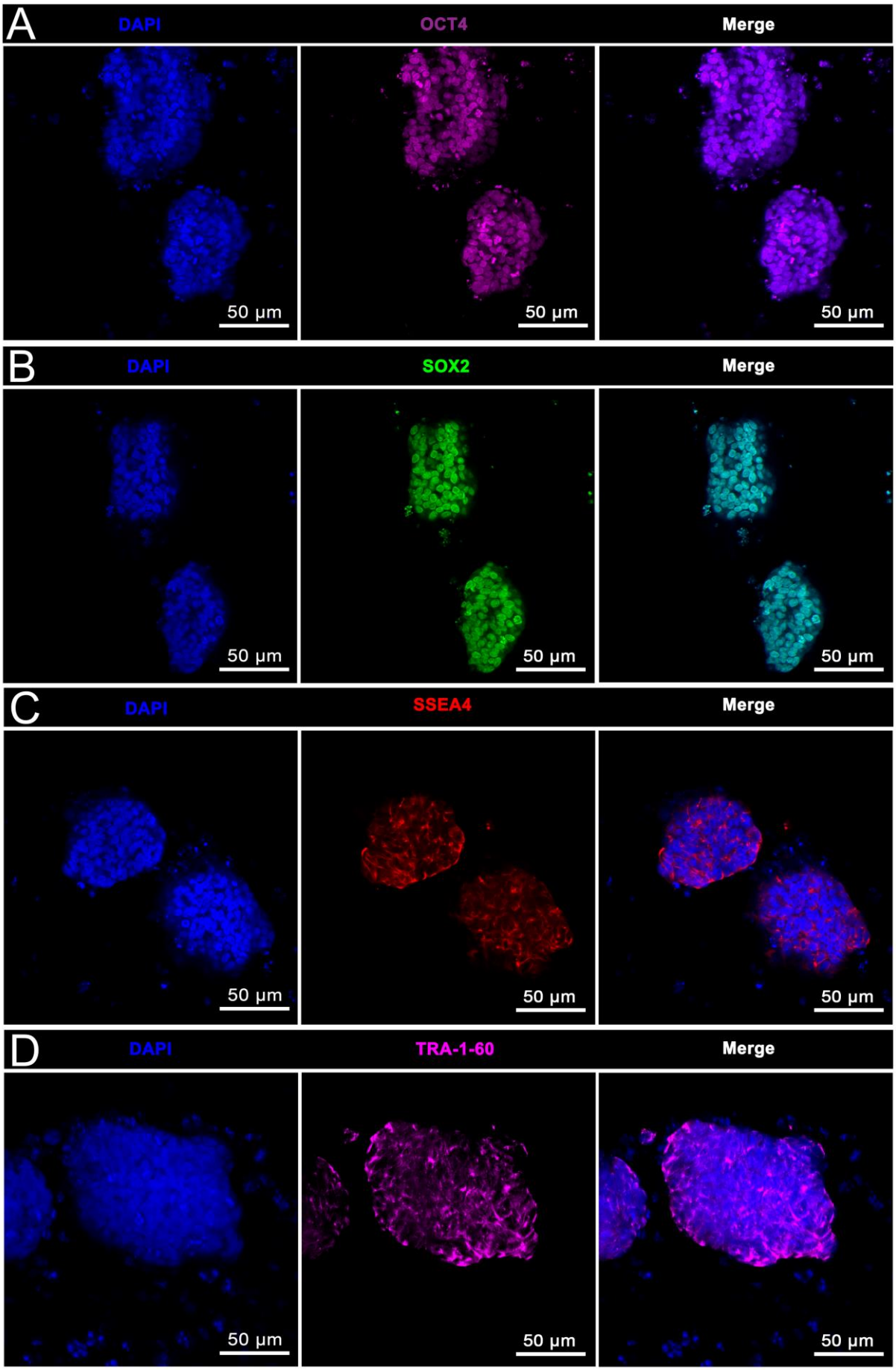
A
DAPI
OCT4
Merge
50 µm
50 µm
50 µm
B
DAPI
SOX2
Merge
50 µm
50 µm
50 µm
C
DAPI
SSEA4
Merge
50 µm
50 µm
50 µm
D
DAPI
TRA-1-60
Merge
50 µm
50 µm
50 µm

Figure 3. Immunophenotyping of 3D bioprinted human iPSCs 10 days post-printing. iPSCs formed spheroids, stained with DAPI, and expressed pluripotency markers A) OCT4, B) SOX2, C) SSEA4, and D) TRA-1-60. Pseudocoloured images as indicated by colour of text. Scale bars as indicated.

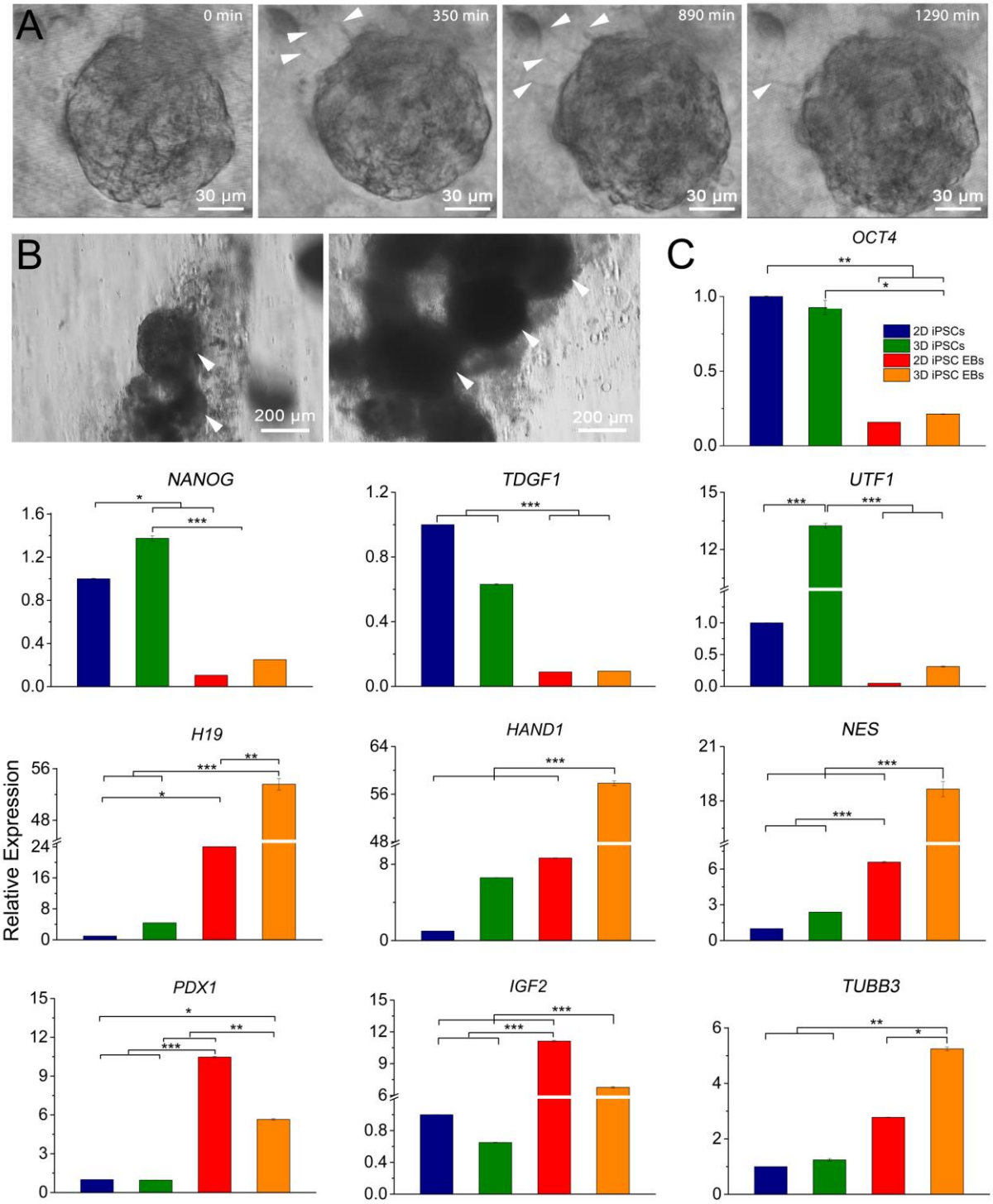

Figure 4. *In situ* formation of EBs from 3D bioprinted human iPSCs 15 days post-printing (including 10 days iPSC differentiation). A) EBs formed within 3D constructs, displayed typical morphology, with elongated cell projections resembling neurite extensions radiating out and retracting over time (arrowheads; See also Video S1, Supporting Information). B) EBs within 3D constructs (arrowheads) were extracted for RT-qPCR. C) Comparative gene expression (*OCT4*, *NANOG*, *TDGF1* and *UTF1*: pluripotency markers; *H19* and *PDX1*:

endodermal markers; *Hand-1* and *IGF2*: mesodermal markers; *NES* and *TUBB3*: ectodermal markers) between conventional 2D and 3D iPSCs and EBs. Relative gene expression represents data normalized to *β*-actin (ACTB) and expressed relative to 2D iPSCs. Mean ± S.D.; *n* = 3. One-way Anova with Bonferroni post hoc test. **P*< 0.05; ** *P*< 0.01; *** *P*< 0.001. Scale bars as indicated.

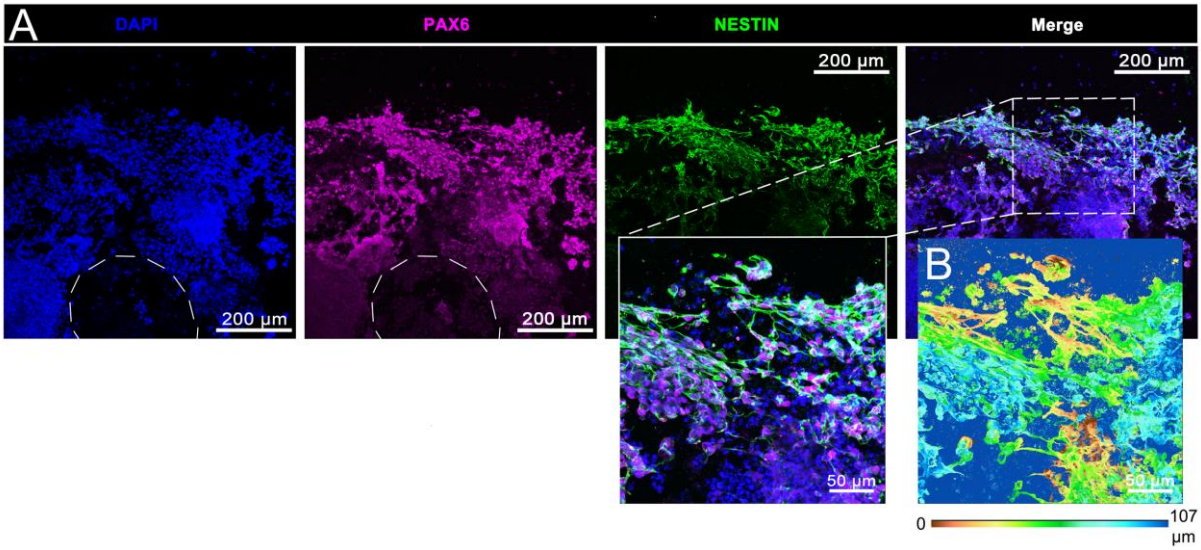

Figure 5. Immunophenotyping of 3D bioprinted human iPSCs 20 days post-printing including 17 days of neural induction. A) Cells stained with DAPI and expressed neural progenitor markers PAX6 and nestin. B) Depth coding of cells along the Z-axis of a 3D printed construct (0 – 107 µm). Pseudocoloured images as indicated by colour of text. White dashed lines of DAPI and PAX6 labelling images outline the lumen of printed scaffold/construct. Scale bars as indicated.

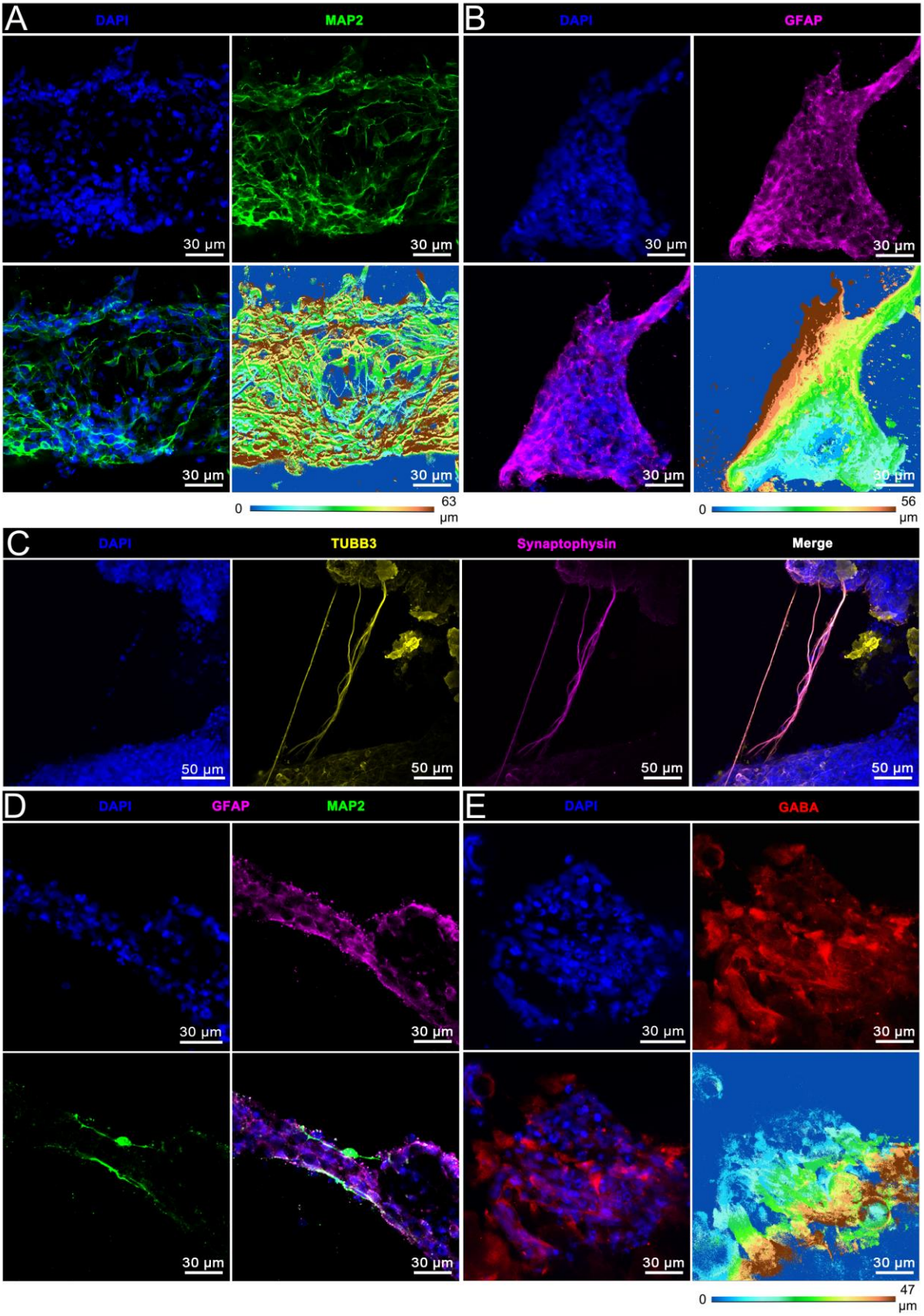

Figure 6. Immunophenotyping of 3D bioprinted human iPSCs 40 days post-printing including 30-37 days of neural induction and differentiation. A) Cells stained with DAPI and expressed pan-neuronal marker MAP2 revealing neural processes extending throughout constructs, as well as B) radial glia and astrocyte marker GFAP. Also shown, depth coding of

cells along the Z-axis 0 – 63 µm and 0 – 56 µm respectively. C) Cells stained with DAPI and pan neuronal-marker TUBB3. Synaptophysin colocalized with TUBB3-labelled processes extending between neuronal cell clusters. D) MAP2 expressing neurons with neurites abutting and partially colocalized with GFAP expressing glial cells. E) GABAergic subtype neurons expressing GABA. Also, depth coding of cells along the Z-axis 0 – 47 µm. Pseudocoloured images as indicated by colour of text. Scale bars as indicated.

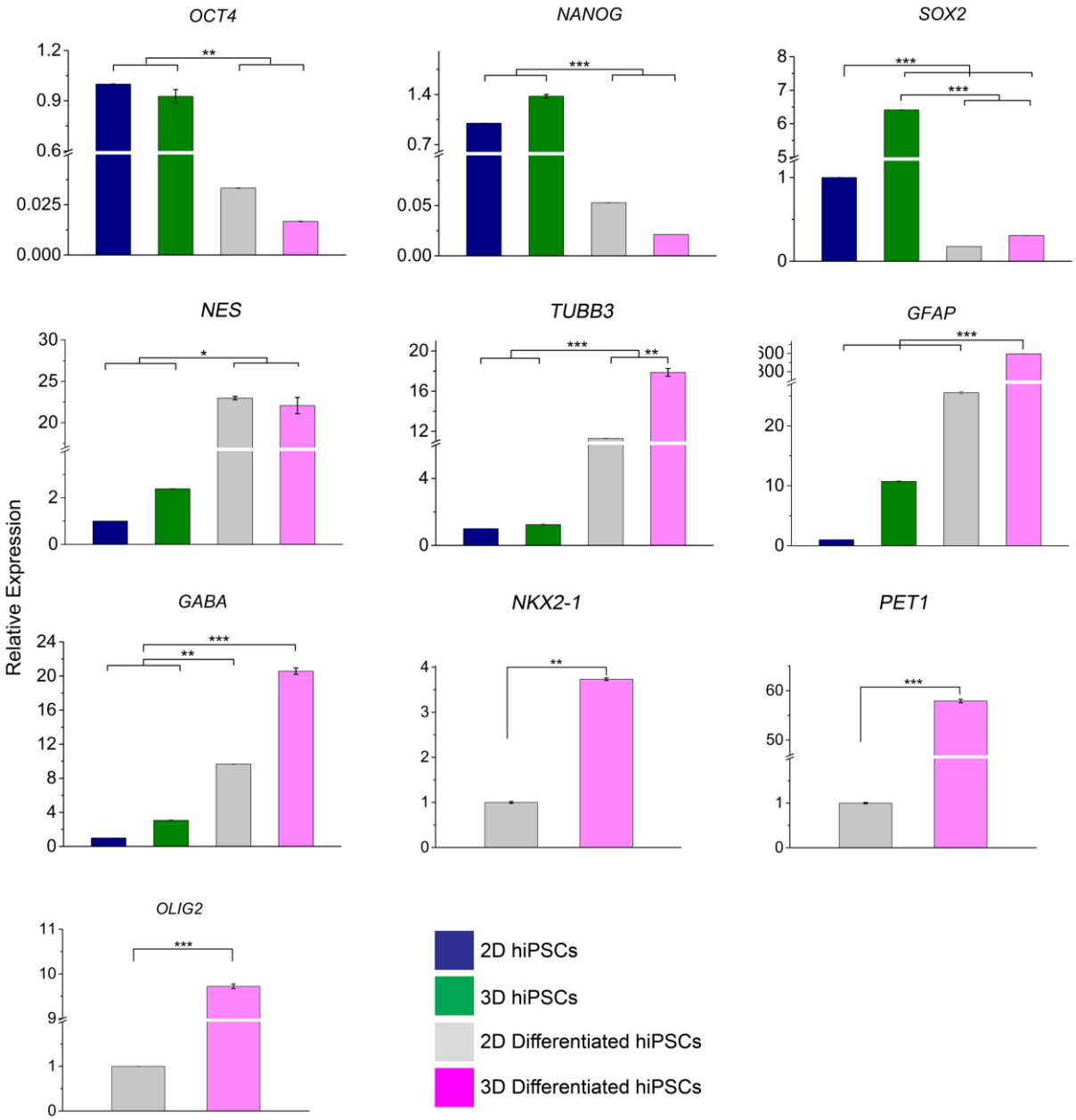

Figure 7. Comparative gene expression (pluripotency: *OCT4*, *NANOG*, *SOX2*; neural: *NES*, *TUBB3*, *GFAP*, *GABA*, *NKX2-1*, *PET1*, *OLIG2*) between conventional 2D and 3D (bioprinted) hiPSC and neural derivative cultures. Mean ± S.D.; n = 3. One-way Anova with Bonferroni post hoc test or Student's t-test. *P< 0.05; ** P< 0.01; *** P< 0.001.

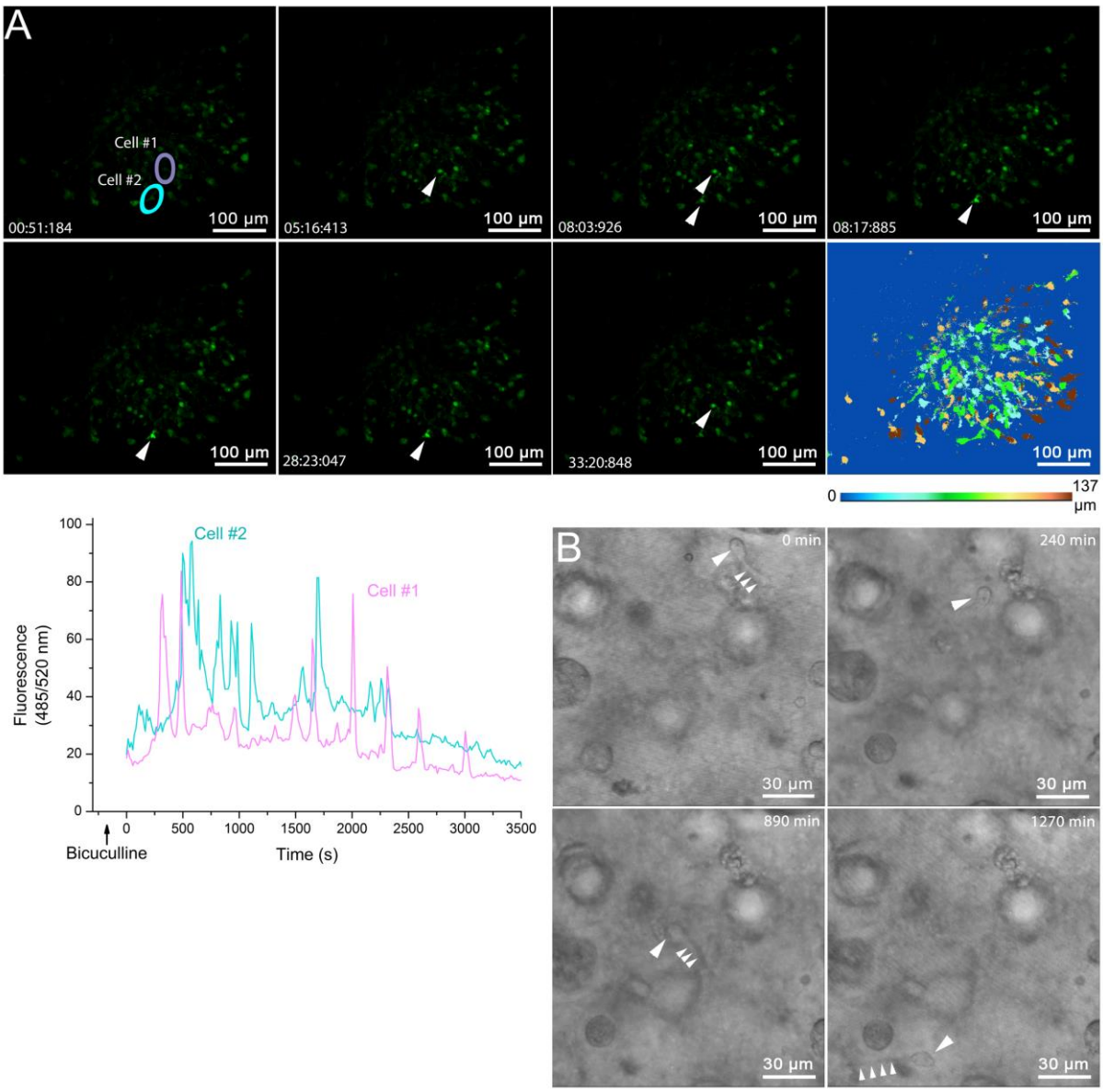

Figure 8. Live cell imaging of calcium flux and cell migration showing functional neurons forming networks within 3D structures 40 days after printing iPSCs including 37 days of neural induction and differentiation. A) Time course of bicuculline-induced calcium flux for individual neurons 1-2 within a 3D construct (arrowheads; See also Video S2, Supporting Information). The photomicrographs and corresponding line-plots show active cells (arrowheads) and average measurements of calcium flux respectively. Also shown, depth coding of cells along the Z-axis of the 3D printed construct (0 – 137 µm). B) Live cell imaging demonstrating neuronal cell migration within a 3D construct (large arrowheads: cell soma; small arrowheads: leading process). (See also Video S3, Supporting Information). Pseudocoloured images as indicated by colour of text. Scale bars as indicated.

The table of contents entry: Human tissues are generated by 3D bioprinting human induced pluripotent stem cells that proliferate and differentiate to form renewable 3D tissues. 3D tissues comprise cells of the three germ lineages – endoderm, ectoderm and mesoderm, demonstrating the capacity to form all cells and tissues of the body, or more homogeneous neural tissues containing functional (including migrating) neurons and supporting neuroglia.

Keyword: 3D bioprinting, induced pluripotent stem cells, endoderm, ectoderm, mesoderm, neural tissue

Qi Gu, Eva Tomaskovic-Crook, Gordon G. Wallace*, and Jeremy M. Crook*

Title: 3D Bioprinting human induced pluripotent stem cell constructs for *in situ* cell proliferation and successive multi-lineage differentiation

ToC figure: